



HAL
open science

Platonic topology and CMB fluctuations: homotopy, anisotropy and multipole selection rules

Peter Kramer

► **To cite this version:**

Peter Kramer. Platonic topology and CMB fluctuations: homotopy, anisotropy and multipole selection rules. *Classical and Quantum Gravity*, 2010, 27 (9), pp.95013. 10.1088/0264-9381/27/9/095013 . hal-00591190

HAL Id: hal-00591190

<https://hal.science/hal-00591190>

Submitted on 7 May 2011

HAL is a multi-disciplinary open access archive for the deposit and dissemination of scientific research documents, whether they are published or not. The documents may come from teaching and research institutions in France or abroad, or from public or private research centers.

L'archive ouverte pluridisciplinaire **HAL**, est destinée au dépôt et à la diffusion de documents scientifiques de niveau recherche, publiés ou non, émanant des établissements d'enseignement et de recherche français ou étrangers, des laboratoires publics ou privés.

Platonic topology and CMB fluctuations: Homotopy, anisotropy, and multipole selection rules.

Peter Kramer,
Institut für Theoretische Physik der Universität Tübingen,
Germany.

January 24, 2010

Abstract.

The Cosmic Microwave Background CMB originates from an early stage in the history of the universe. Observations show low multipole contributions of CMB fluctuations. A possible explanation is given by a non-trivial topology of the universe and has motivated the search for topological selection rules. Harmonic analysis on a topological manifold must provide basis sets for all functions compatible with a given topology and so is needed to model the CMB fluctuations. We analyze the fundamental groups of Platonic tetrahedral, cubic, and octahedral manifolds using deck transformations. From them we construct the appropriate harmonic analysis and boundary conditions. We provide the algebraic means for modelling the multipole expansion of incoming CMB radiation. From the assumption of randomness we derive selection rules, depending on the point symmetry of the manifold.

1 Introduction.

Temperature fluctuations of the incoming Cosmic Microwave Background, originating from an early state of the universe, are being studied with great precision. We refer to [12] for the data. The weakness of the observed amplitudes for low multipole orders, see for example [8], was taken by various authors as a motivation to explore constraints on the multipole amplitudes coming from non-trivial topologies of the universe. The topology of the universe is not fixed by the differential equations of Einstein's theory of gravitation. It has been suggested that specific topological models lead to the selection and exclusion of certain low multipole moments and might explain the observations. Harmonic analysis provides a basis set for all functions compatible with a given topology. The general idea is to model the amplitude of incoming CMB radiation by these basis functions. Since the observations provide multipole expansion in two angular coordinates, we discuss the reduction from the three variables on the 3-sphere to the observer frame.

The authors of [24], [21] survey general topological concepts and give particular examples applied to cosmology. For representative contributions by other authors, we quote [24], [23], [25], [1], [2], [3], [30], [4], [31], [5], and references given in these papers. In contrast to the previous numerical work, we give analytical expressions for the basis sets. As most of these authors we assume average positive curvature and so analyze spherical 3-manifolds. Spherical 3-manifolds come in families, one of particular interest being the class of Platonic polyhedra (see i.e. the dodecahedron in [30, 16]). Here we present a systematic approach to the Platonic polyhedra, based on new insight into the homotopy [11], which enables us to characterize new topologies. In the present work, we construct for these topologies the harmonic analysis and provide the algebraic tools for modelling the multipole expansion of CMB fluctuations.

In section 2 we discuss our general methods. In section 3 we set the coordinates and introduce the Wigner polynomials. In section 4 we describe the harmonic analysis on seven spherical Platonic 3-manifolds. We demonstrate and illuminate in section 5 the map from homotopies to deck transformations for cubic 3-manifolds and the homotopic boundary conditions. In section 6 we set the algebraic tools for the modelization of the CMB and then prove multipole selection rules for randomly chosen functions. The novel points of the present analysis are summarized in section 7. Three Appendices deal with A the details of seven Platonic manifolds, B the Wigner polynomials, and C random point symmetry.

2 From homotopy to harmonic analysis on a manifold.

We now examine how the fundamental group determines the analysis of functions on a manifold. The topology of a manifold \mathcal{M} is characterized by its homotopy. For general notions of topology we refer to [27] and [29]. The fundamental or first homotopy group $\pi_1(\mathcal{M})$ of a manifold \mathcal{M} has as its elements inequivalent classes of continuous paths on the manifold \mathcal{M} , returning to the same point. Group multiplication is given by path concatenation.

The simply connected universal cover of a manifold offers another view. This cover, for spherical 3-manifolds the 3-sphere S^3 , is tiled by copies of \mathcal{M} . The tiling is produced by the fixpoint-free action of a group H . The discrete groups acting fixpoint-free on covers are called space forms. The general classification of spherical space forms of low dimension is given by Wolf [33] pp. 224-226.

For cosmic topology, these groups acting on S^3 are taken as the starting point in [23] and [1]. These and other authors choose actions of these groups on S^3 and compute by numerical methods [1], or with the help of the Laplacian [23], corresponding eigenmodes. It is assumed that the groups H are isomorphic to the fundamental group of a manifold. We do not follow this route since there is no unique pathway from the bare group H back to the manifold \mathcal{M} , its geometric boundaries and homotopies. First of all, from eq. 9, and as noted in [23] pp. 4686-4687, the unitary unimodular group $SU(2, C)$, and so any of its discrete subgroups, admits at least three different types of actions on S^3 . Moreover, cyclic

groups $H = C_n$, denoted in [23] as Z_n and associated there on pp. 4688 with lens space manifolds, emerge in our analysis as C_5 for the tetrahedral manifold $N1$ and as C_8 for the cubic manifold $N3$. It follows that a bare cyclic group acting on S^3 does not determine a unique topological manifold.

Instead we follow [27] and take the manifold and its fundamental group of homotopies as our starting point. The group H that generates the tiling on the cover we call with [27] the group of deck transformations $H = \text{deck}(\mathcal{M})$. Homotopy and deck transformations are linked together in a theorem due to Seifert and Threlfall [27] pp. 196-198. It states that, for a manifold \mathcal{M} , the group of deck transformations and the fundamental group of homotopies are isomorphic.

For polyhedral manifolds, homotopies are generated by the gluing of boundaries. Everitt in [11] determines (with minor corrections given in [6]), all possible homotopies of the family of Platonic polyhedra on S^3 . The theorem by Seifert and Threlfall ensures that from any face gluing generator of a polyhedral homotopy one can find an associated deck transformation that maps on S^3 a prototile to a neighbouring image tile. We implement this theorem and construct, on the basis of work detailed in [16], [18], [19], [20], from homotopic face gluings the isomorphic generators of deck transformations. In this way we derive from homotopies, rather than postulate, the individual groups H of deck transformations and at the same time obtain definite actions of them on S^3 .

The constructed group $H = \text{deck}(\mathcal{M})$ is our key to the analysis of functions on the manifold. Harmonic analysis on S^3 , with the domain being a spherical 3-manifold, is the exact spherical counterpart of Euclidean crystallographic Fourier series analysis. In fact, the analysis of Euclidean cosmic topology given in [3] exemplifies crystallographic analysis for topology with Euclidean cover. On S^3 , we start from the Wigner polynomials since they span an orthonormal harmonic basis for square integrable functions. By algebraic projection and multiplicity analysis we construct for each Platonic manifold all H -invariant linear combinations of Wigner polynomials. These in turn span a basis that respects the tiling, incorporates the fundamental group, and has the spherical manifold as its domain. From our analysis there follow strict boundary conditions, set by homotopy, on pairs of faces of the spherical polyhedron.

3 The 3-sphere, its isometries, and Wigner polynomial bases.

Our starting point for the functional analysis on spherical manifolds are the 3-sphere, its coordinates, and an orthogonal system of harmonic polynomials on it. The points of the 3-sphere are in one-to-one correspondence to the elements of the unitary unimodular group $SU(2, C)$. This allows to choose coordinates on the 3-sphere. We label them by a 2×2 unimodular matrix in the form

$$u = \begin{bmatrix} z_1 & z_2 \\ -\bar{z}_2 & z_1 \end{bmatrix}, \quad z_1 = x_0 - ix_3, \quad z_2 = -x_2 - ix_1, \quad z_1\bar{z}_1 + z_2\bar{z}_2 = 1. \quad (1)$$

where the real coordinates of E^4 are $x = (x_0, x_1, x_2, x_3)$. The group of isometries of S^3 is $SO(4, R)$. This group can be expressed as the direct product of two groups $SU^l(2, C)$, $SU^r(2, C)$ in the form

$$SO(4, R) \sim (SU^l(2, C) \times SU^r(2, C))/Z_2. \quad (2)$$

The action of these groups on $u \in S^3$ is given by

$$(g_l, g_r) \in (SU^l(2, C) \times SU^r(2, C)) : u \rightarrow g_l^{-1} u g_r. \quad (3)$$

The subgroup Z_2 in eq. 2 is generated by $(g_l, g_r) = (-e, -e) \in (SU^l(2, C) \times SU^r(2, C))$. The diagonal subgroup in eq. 2 with elements $(g, g) \in (SU^l(2, C) \times SU^r(2, C))$ we denote by $SU^C(2, C)$. The actions of $SU^C(2, C)$ on u produce rotations $R(g)$ wrt. the three coordinates (x_1, x_2, x_3) . Any element of $SO(4, R)$ can be uniquely factorized as

$$\begin{aligned} (g_l, g'_r) &= (g_l, g_l)(e, g_r), \quad g_r := g_l^{-1} g'_r, \\ (g_l, g_l) &\in SU^C(2, C), \quad (e, g_r) \in SU^r(2, C). \end{aligned} \quad (4)$$

These relations express the fact that the points of the coset space $SO(4, R)/SU^C(2, C)$ can be identified with the elements of $SU^r(2, C)$, and hence with the points of the 3-sphere S^3 . The 4-dimensional spherical harmonics have this coset space as their domain. As shown in [18], these spherical harmonics can be identified with the Wigner D^j -functions

$$D^j_{m_1, m_2}(u), \quad 2j = 0, 1, \dots, \infty, \quad -j \leq (m_1, m_2) \leq j. \quad (5)$$

Wigner [32] pp. 166-170 introduced them as the unitary irreducible representations of the group $SU(2, C)$, often parametrized by three Euler angles eq. 12. Since the Wigner D^j functions can be seen as a complete orthogonal system of polynomial functions on S^3 , homogeneous of degree $2j$ in the four complex matrix elements of u , see Appendix B, we coin for them the name Wigner polynomials. As shown in [18] Lemma 5 p. 3526, these polynomials are harmonic, i.e. vanish under application of the Laplacian in E^4 , eq. 48. The action of a general element $(g_l, g_r) \in (SU^l(2, C) \times SU^r(2, C))$ on a spherical harmonic eq. 5 is given, using the representation properties of D^j , by

$$\begin{aligned} (T_{(g_l, g_r)} D^j_{m_1, m_2})(u) &:= D^j_{m_1, m_2}(g_l^{-1} u g_r) \\ &= \sum_{(m'_1, m'_2)=-j}^j D^j_{m'_1, m'_2}(u) \left[D^j_{m_1, m'_1}(g_l^{-1}) D^j_{m'_2, m_2}(g_r) \right], \end{aligned} \quad (6)$$

in terms of products of two Wigner D^j -functions of the acting group elements (g_l, g_r) . It follows that the 3-sphere supports both the action of the group H and the H -invariant basis of the harmonic analysis. Moreover, it allows to compare spherical topologies with different homotopies, groups H , and harmonic analysis.

3.1 Projection and multiplicity for H -invariant polynomials.

Given the group H of deck transformations, we can project on the chosen manifold a basis for the harmonic analysis. The projector P^0 from a Wigner to a H -invariant polynomial produces, using eq. 6, the linear combination

$$(P^0 D_{m_1 m_2}^j)(u) = \sum_{m'_1 m'_2} D_{m'_1 m'_2}^j(u) \left[\frac{1}{|H|} \sum_{(g_l, g_r) \in H} D_{m_1 m'_1}^j(g_l^{-1}) D_{m'_2 m_2}^j(g_r) \right]. \quad (7)$$

By standard methods of group representations, the multiplicity $m(j, 0)$ of linear independent H -invariant polynomials for given j is, from computing the characters of the representation eq. 6, given by

$$m(j, 0) = \frac{1}{|H|} \sum_{(g_l, g_r) \in H} \chi^j(g_l^{-1}) \chi^j(g_r), \quad (8)$$

with $\chi^j(g)$ the character [32] pp. 155-156 of $g \in SU(2, C)$ and $|H|$ the order of H . The multiplicity eq. 8 controls the number of linearly independent projections eq. 7.

3.2 Boundary conditions for the harmonic analysis set by the homotopy group H .

For a given polyhedral shape, the first homotopy group H is generated by the gluing of pairs of faces. The isomorphic map of homotopies to deck transformations is sketched in section 2 and carried out in our previous work. Now pairs of faces glued by homotopy appear in the tiling generated by deck transformations as boundaries shared by pairs of neighbouring polyhedral tiles. This map and the boundary conditions are demonstrated in 5. There follows

Prop 1: Any H -invariant polynomial, defined on the polyhedron, must repeat its values on pairs of faces of the prototile linked by the elements of $H = \text{deck}(\mathcal{M})$ isomorphic to the homotopic gluing of faces.

The harmonic analysis on the polyhedral prototile therefore is subject to these boundary conditions. Homotopies from the same polyhedral shape are distinguished by their boundary conditions. Moreover, since the underlying Wigner polynomials are harmonic, we have

Prop 2: The H -invariant polynomials on a polyhedron solve the Laplace equation inside the polyhedron. Their values are repeated on pairs of faces, related by the face gluings from the group H of homotopies.

Coxeter diagram Γ	$ \Gamma $	Polyhedron \mathcal{M}	$H = \text{deck}(\mathcal{M})$	$ H $	Reference
$\circ - \circ - \circ - \circ$	120	tetrahedron $N1$	C_5	5	[18]
$\overset{4}{\circ - \circ - \circ - \circ}$	384	cube $N2$ cube $N3$	C_8 Q	8 8	[19] [19]
$\overset{4}{\circ - \circ - \circ - \circ}$	1152	octahedron $N4$ octahedron $N5$ octahedron $N6$	$C_3 \times Q$ B \mathcal{T}^*	24 24 24	[20] [20] [20]
$\overset{5}{\circ - \circ - \circ - \circ}$	$120 \cdot 120$	dodecahedron $N1'$	\mathcal{J}^*	120	[16], [17]

Table 1: 4 Coxeter groups Γ , 4 Platonic polyhedra \mathcal{M} , 7 groups $H = \text{deck}(\mathcal{M})$ of order $|H|$. In the Table, C_n denotes a cyclic, Q the quaternion, \mathcal{T}^* the binary tetrahedral, \mathcal{J}^* the binary icosahedral group. The symbols Ni are adapted from [11].

4 Platonic 3-manifolds, groups of deck transformations, and bases for the harmonic analysis.

4.1 Coxeter groups on the 3-sphere and Platonic polyhedra.

To construct the Platonic 3-manifolds we follow [11] and introduce Coxeter groups Γ generated by reflections in hyperplanes of E^4 . One reason for their use is that all faces of the Platonic polyhedra are located on such reflection hyperplanes. Moreover the Platonic tilings of S^3 can be found from the defining representations on E^4 of these groups. We shall use in subsection 4.2 the representations of the Coxeter groups to construct the deck transformations. In section 6 we shall use these Coxeter groups to discuss the random point symmetry of the manifolds.

Given Euclidean space with standard scalar product \langle, \rangle , a Weyl reflection W_a with unit Weyl vector $a : \langle a, a \rangle = 1$ acts on $x \in E^4$ as

$$W_a : x \rightarrow W_a x := x - 2\langle x, a \rangle a, (W_a)^2 = e. \quad (9)$$

This is a reflection in the hyperplane perpendicular to the unit vector a . Coxeter groups Γ [13] are generated by Weyl reflections with relations of the type $(W_{a_i} W_{a_j})^{m_{ij}} = e$. The Coxeter diagram encodes Weyl reflections by nodes, and by integer numbers m_{ij} for relations of pairs of generating Weyl reflections. A horizontal line in the diagram between two nodes denotes the particular value $m_{ij} = 3$. The numbers m_{ij} determine also the scalar products between the corresponding pairs of Weyl unit vectors by

$$\langle a_i, a_j \rangle = \cos\left(\frac{\pi}{m_{ij}}\right). \quad (10)$$

Pairs of unlinked nodes in the Coxeter diagram yield Weyl reflection vectors perpendicular to one another and reflections that commute.

Γ	a_1	a_2	a_3	a_4
$\circ - \circ - \circ - \circ$	$(0, 0, 0, 1)$	$(0, 0, \sqrt{\frac{3}{4}}, \frac{1}{2})$	$(0, \sqrt{\frac{2}{3}}, \sqrt{\frac{1}{3}}, 0)$	$(\sqrt{\frac{5}{8}}, \sqrt{\frac{3}{8}}, 0, 0)$
$\overset{4}{\circ - \circ - \circ - \circ}$	$(0, 0, 0, 1)$	$(0, 0, -\sqrt{\frac{1}{2}}, \sqrt{\frac{1}{2}})$	$(0, \sqrt{\frac{1}{2}}, -\sqrt{\frac{1}{2}}, 0)$	$(-\sqrt{\frac{1}{2}}, \sqrt{\frac{1}{2}}, 0, 0)$
$\circ - \overset{4}{\circ - \circ - \circ}$	$(0, \sqrt{\frac{1}{2}}, -\sqrt{\frac{1}{2}}, 0)$	$(0, 0, -\sqrt{\frac{1}{2}}, \sqrt{\frac{1}{2}})$	$(0, 0, 0, 1)$	$(\frac{1}{2}, \frac{1}{2}, \frac{1}{2}, \frac{1}{2})$
$\circ - \circ - \overset{5}{\circ - \circ}$	$(0, 0, 1, 0)$	$(0, -\frac{\sqrt{-\tau+3}}{2}, \frac{\tau}{2}, 0)$	$(0, -\sqrt{\frac{\tau+2}{5}}, 0, -\sqrt{\frac{-\tau+3}{5}})$	$(\frac{\sqrt{2-\tau}}{2}, 0, 0, -\frac{\sqrt{\tau+2}}{2})$

Table 2: The Weyl vectors a_s for the four Coxeter groups Γ from Table 1 with $\tau := \frac{1+\sqrt{5}}{2}$.

The Platonic polyhedra in 3 dimensions form a family of regular polyhedra, bounded by the regular 2-dimensional polygons. Similarly, the m-cells, see [28], are a family of regular polyhedra in 4 dimensions, bounded by the regular 3-dimensional Platonic polyhedra. By projection of the Euclidean geometric objects to the spheres S^2 and S^3 respectively, one obtains spherical polygons, polyhedra and m-cells. The geometric symmetry of these objects we express in terms of 4 Coxeter reflection groups Γ . Their diagrams are given in Table 1 and their four generators in Table 2. For a fixed Coxeter group we use the short-hand notation $\Gamma : W_{a_j} =: W_i$.

The Weyl reflection planes of the first three generators of Γ pass through the point $(1, 0, 0, 0)$ and bound a cone. The intersection of this cone with the Weyl reflection plane of the fourth generator bounds what is called the Coxeter simplex. Each of the Coxeter groups Γ tiles S^3 into $|\Gamma|$ copies of a fundamental Coxeter simplex. In topology we are interested in actions preserving orientation. The maximal subgroup of a Coxeter group with this property is generated by the products $(W_1W_2), (W_2W_3), (W_3W_4)$ of generators. Its representation on E^4 is given by unimodular matrices with determinant 1. Because of its unimodular representation we denote this subgroup by $S\Gamma$, and find for its order $|S\Gamma| = |\Gamma|/2$. The fundamental domain for $S\Gamma$ can be taken as a duplex, formed by a mirror pair of Coxeter simplices.

The Platonic polyhedra are built from sets of Coxeter simplices sharing a single vertex, as illustrated in Figs. 2-8.

The group $H = \text{deck}(\mathcal{M})$ is a subgroup of Γ and produces on S^3 a second, superimposed tiling by $|H|$ copies of a Platonic polyhedron \mathcal{M} . Since $|H|$ must be equal to m , the tiling is a $|H|$ -cell on S^3 . The Platonic $|H|$ -cells are discussed and illustrated in [28].

The Platonic polyhedra become topological 3-manifolds upon specifying fundamental groups or homotopies for them as is done in [11]. We adopt the notation N_j for these manifolds. Note from section 5 that a single polyhedral shape can carry several inequivalent fundamental groups of equal order. For a list of the non-abelian groups of order ≤ 30 we refer to [9] pp. 134-135, Table 1. Binary symmetry groups, given as subgroups of $SU(2, C)$, we denote by a star *.

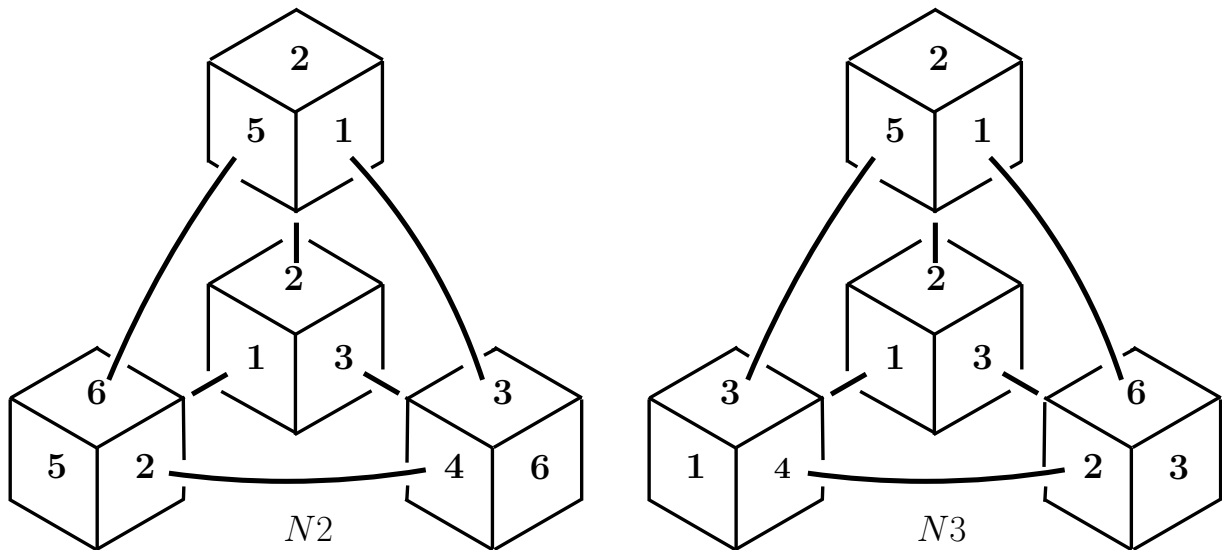


Figure 1: The cubic manifolds $N2$ and $N3$. The cubic prototile and three neighbour tiles sharing its faces $F1, F2, F3$. The four cubes are replaced by their Euclidean counterparts and separated from one another. Visible faces are denoted by the numbers from Fig. 6. The actions transforming the prototile into its three neighbours generate the deck transformations and the 8-cell tiling of S^3 . In the tiling, homotopic face gluing takes the form of shared pairs of faces $N2 : F3 \cup F1, F4 \cup F2, F6 \cup F5$ and $N3 : F1 \cup F6, F2 \cup F4, F3 \cup F5$. It is marked by heavy lines or arcs.

4.2 Representation of products of Weyl reflections.

We shall construct the deck transformations of the Platonic polyhedra from even products of Weyl reflections. Here we provide the appropriate algebraic tools. For a Weyl reflection with Weyl unit vector a_s , we define the 2×2 matrix v_s by inserting the four Cartesian components of a_s into eq. 1. The product $(W_{a_i} W_{a_j})$ is a rotation in E^4 . The corresponding rotation operator from [18] eq.(60) can be written in terms of the matrices (v_i, v_j) as

$$T_{(W_{a_i} W_{a_j})} = T_{(v_i v_j^{-1}, v_i^{-1} v_j)}, \quad (11)$$

and for fixed degree $2j$ has the representation given in eq. 6. All deck transformations appearing in what follows are orientation-preserving and therefore must be products of an even number of Weyl reflections. Eq. 11 guarantees that all of them can be expressed by pairs (g_l, g_r) .

5 The two spherical cubic manifolds.

In this section we illustrate the use of the cover S^3 and of deck transformations by two spherical cubic 3-manifolds. They are the spherical counterparts of the Euclidean cubic

manifold discussed in [3]. Everitt in [11] constructs two inequivalent cubic manifolds which we denote by $N2, N3$. His face and edge gluings are given in section A.2. These we illustrate in Fig. 1. All spherical cubes are replaced by their Euclidean counterparts. We start from the cubic prototile and the homotopic gluing of its faces, enumerated as $F1, F2, F3$ according to Fig. 6. These gluings we transform in A.2 into deck transformations from the prototile to its three neighbour tiles, shown separated with parallel faces in the Figure. When passing to S^3 , the Euclidean cubes are replaced by spherical cubes of the cubic 8-cell tiling of S^3 , see [28] p. 177-8 and [19] Fig. 1. The enumeration of the visible faces in the figure shows that they have been rotated. In the 8-cell tiling of S^3 , the homotopic gluing appears as the sharing of faces. In the figure we connect pairs of shared faces by heavy lines or arcs. The differences between the left $N2$ and right $N3$ manifold illustrates the two inequivalent fundamental groups found in [11], both with the same cubic shape of the prototile. The corresponding groups H of deck transformations we construct algebraically in A.2 as a cyclic group $H = C_8$ for $N2$ and the quaternion group $H = Q$ for $N3$, both of order 8. The bases of the harmonic analysis on the two cubic manifolds we find by algebraic projection as H -invariant linear combinations of Wigner polynomials. They are listed in subsection A.2. Their values on the prototile differ in their homotopic boundary conditions. Therefore we expect for them in general different anisotropies and multipole expansions.

6 Modelling incoming CMB by harmonic analysis.

In this section we discuss the algebraic tools for analysing incoming CMB radiation in terms of the harmonic bases for a chosen topology.

6.1 Alternative coordinates on S^3 .

For the harmonic analysis on spherical 3-manifolds we use the spherical harmonics in the form of Wigner polynomials. These polynomials in the coordinates x are often expressed in terms of Euler angle coordinates, Edmonds [10] pp. 53-67:

$$\begin{array}{l}
 \boxed{
 \begin{array}{l}
 x_0 = \cos\left(\frac{\alpha+\gamma}{2}\right) \cos\left(\frac{\beta}{2}\right), \quad x_1 = -\sin\left(\frac{\alpha-\gamma}{2}\right) \sin\left(\frac{\beta}{2}\right), \\
 x_2 = -\cos\left(\frac{\alpha-\gamma}{2}\right) \sin\left(\frac{\beta}{2}\right), \quad x_3 = -\sin\left(\frac{\alpha+\gamma}{2}\right) \cos\left(\frac{\beta}{2}\right),
 \end{array}
 } \\
 u = \left[\begin{array}{cc}
 \exp\left(\frac{i(\alpha+\gamma)}{2}\right) \cos\left(\frac{\beta}{2}\right), & \exp\left(\frac{i(\alpha-\gamma)}{2}\right) \sin\left(\frac{\beta}{2}\right) \\
 \exp\left(\frac{i(-\alpha+\gamma)}{2}\right) \sin\left(\frac{\beta}{2}\right), & \exp\left(\frac{-i(\alpha+\gamma)}{2}\right) \cos\left(\frac{\beta}{2}\right)
 \end{array} \right]
 \end{array} \tag{12}$$

We give the coordinates and the form of the matrix u eq. 1. An alternative system of polar coordinates is used by Aurich et al. [1]. Here

$$\begin{array}{l}
 x_0 = \cos(\chi), \quad x_1 = \sin(\chi) \sin(\theta) \cos(\phi), \\
 x_2 = \sin(\chi) \sin(\theta) \sin(\phi), \quad x_3 = \sin(\chi) \cos(\theta), \\
 \\
 u = \begin{bmatrix} \cos(\chi) - i \sin(\chi) \cos(\theta), & -i \sin(\chi) \sin(\theta) \exp(-i\phi) \\ -i \sin(\chi) \sin(\theta) \exp(i\phi), & \cos(\chi) + i \sin(\chi) \cos(\theta) \end{bmatrix}
 \end{array} \tag{13}$$

We shall see in eq. 18 that these polar coordinates are adapted to the analysis of incoming radiation in terms of its direction.

6.2 Multipole expansion of spherical harmonics on S^3 .

For a clear description of the multipole analysis of the CMB we refer to [1]. We relate our analysis algebraically to this description. The Wigner polynomials eq. 46 in Euler angle coordinates eq. 12 from [10] p. 55 factorize as

$$D_{m_1, m_2}^j(u) = \exp(im_1\alpha) d_{m_1, m_2}^j(\beta) \exp(im_2\gamma) \tag{14}$$

To adapt the Wigner polynomials to a multipole expansion, we transform them for fixed degree $2j$ by use of Wigner coefficients of $SU(2, C)$, [10] pp. 31-45, into the new harmonic polynomials

$$\begin{aligned}
 \psi_{\beta lm}(u) &= \delta_{\beta, 2j+1} \sum_{m_1, m_2} D_{m_1, m_2}^j(u) \langle j - m_1, j, m_2 | lm \rangle (-1)^{j-m_1}, \\
 l &= 0, 1, \dots, 2j = \beta - 1.
 \end{aligned} \tag{15}$$

This transformation links the Wigner polynomials to the basis given in [1] whose index notation we adopt. Whereas the index j of the Wigner polynomials can be integer or half-integer, the multipole index l takes only integer values. For fixed l we have $2j \geq l$, and for fixed $2j$: $0 \leq l \leq 2j$. Using representation theory of $SU(2)$ it can be shown from eqs. 6 and 15 that the conjugation action $u \rightarrow g^{-1}ug$ of the group $SU^C(2, C)$ acts by a rotation $R(g)$ only on the coordinate triple (x_1, x_2, x_3) , and the new polynomials eq. 15 transform as

$$(T_{(g,g)}\psi_{\beta lm})(u) = \psi_{\beta lm}(g^{-1}ug) = \sum_{m'=-l}^l \psi_{\beta lm'}(u) D_{m', m}^l(g), \tag{16}$$

like the spherical harmonics $Y_m^l(\theta, \phi)$. We therefore adopt eq. 16 as the action of the usual rotation group for cosmological models covered by the 3-sphere. Eq. 16 qualifies l as the multipole index of incoming radiation.

The basis transformation eq. 15 can be inverted with the help of the orthogonality of the Wigner coefficients [10] to yield

$$D_{m_1, m_2}^j(u) = \delta_{\beta, 2j+1} \delta_{m, -m_1+m_2} \sum_{l=0}^{2j} \psi_{\beta l m}(u) \langle j - m_1 j m_2 | l m \rangle (-1)^{j-m_1} \quad (17)$$

The result eq. 16 can be further elaborated by use of the alternative coordinates (χ, θ, ϕ) eq. 13. We follow Aurich et al. [1], eqs. 9-17, to find

$$\begin{aligned} \psi_{\beta l m}(u) &= R_{\beta l}(\chi) Y_m^l(\theta, \phi), \\ R_{\beta l}(\chi) &= 2^{l+\frac{1}{2}} l! \sqrt{\frac{\beta(\beta-l-1)!}{\pi(\beta+l)}} C_{\beta-l-1}^{l+1}(\cos(\chi)) \end{aligned} \quad (18)$$

where $C_{\beta-l-1}^{l+1}$ is a Gegenbauer polynomial. A similar expression is given in [23] pp. 4705-7. Eq. 18 shows that the alternative spherical harmonics eq. 15, written in the polar coordinates eq. 13, admit the separation into a part depending on χ and a standard spherical harmonic as a function of polar coordinates (θ, ϕ) . For a very clear interpretation of the role of the coordinate χ , appearing in the Gegenbauer polynomials of eq. 18, its relation to cosmological models, and to the surface of last scattering, we refer to [1].

6.3 Harmonic analysis and anisotropy from spherical manifolds.

Observed anisotropies of the CMB fluctuations are discussed for example in [34] and [26]. From the present point of view, there are two different sources of anisotropy in the harmonic analysis, which apply to Platonic as well as to other polyhedral topologies.

6.4 Anisotropy from the orientation of the polyhedron.

Although the 3-sphere is isotropic with respect to rotations, any polyhedral prototile has a particular orientation, chosen with the Weyl reflection vectors with respect to the frame of coordinates $x = (x_0, x_1, x_2, x_3)$. For any model derived from a spherical topological manifold, it follows that frames of different orientation on S^3 must be explored independent from one another. There is no motivation for averaging. The most general rotation of the frame of coordinates transforms the Wigner polynomials of fixed degree $2j$ according to eq. 6.

6.5 Anisotropy from the underlying homotopy group.

One way to model the CMB by a given Platonic 3-manifold is to combine its H -invariant basis polynomials, ordered by degree $2j$, linearly with random coefficients, pass with the transformation eq. 17 and coordinate transformation 13 to the new basis eq. 18, consider the dependence on χ mentioned after eq. 18, and evaluate the resulting multipole expansion.

We argue that this general procedure does not ensure simple selection rules for the multipole expansion. The reason is that the full basis must strictly obey the boundary conditions on pairs of faces found from homotopy in section 3.2.

Evidence for the impact of homotopies on the basis of the harmonic analysis is provided in Appendix A by the tetrahedral manifold $N1$, the cubic manifolds $N2, N3$, and by the octahedral manifold $N4$: In all these cases we find new preferred coordinate settings $x' \sim u'$ such that the H -invariant bases become very simple linear combinations of Wigner polynomials $D^j(u')$. These particular coordinate settings from homotopy must produce observable anisotropies.

6.6 Random polyhedral point symmetry and multipole selection rules.

Homotopy implies boundary conditions in the harmonic analysis for pairs of polyhedral faces. These conditions are much weaker than those implied by the geometric rotational point group $M \in SO(3, R)$ of symmetries of the polyhedron. Conversely, the boundary conditions from homotopy do not exclude the geometrical point symmetry of the polyhedron. The compatibility of the point and the deck groups is discussed in Appendix C. We now show that under an additional assumption of randomness there follow multipole selection rules of the type which motivated the search for non-trivial topologies.

M -invariance restricts the domain of a function on a polyhedron to a conal domain of a volume fraction $\frac{1}{|M|}$. For any M -invariant function we have:

Prop 3: If a function, defined on a regular polyhedron, is invariant under its point symmetry group M , it also fulfills the boundary conditions from any of its homotopy groups.

Proof: The action of M on the faces of a regular polyhedron is transitive, i.e. transforms any pair of faces into one another. It also contains the polyhedral rotations preserving the midpoint of any face. Therefore it follows from M -invariance that the boundary values of the function on the faces do obey any homotopic boundary conditions as discussed in section 3.2.

Among possible functions with domain the polyhedron, consider now a random function $\Psi^{\text{random}}(u)$. From eq. 15, any point group element $R(h) \in M$ acts on this random function as

$$(x_1, x_2, x_3) \rightarrow R(h)(x_1, x_2, x_3), u \rightarrow h^{-1}uh, h \in SU^C(2, C). \quad (19)$$

This rotation by assumption preserves the geometrical shape of the manifold, and on it produces a new admissible random function

$$\Psi^{\text{random}}(u) \rightarrow (T_{(h,h)}\Psi^{\text{random}})(u) = \Psi^{\text{random}}(h^{-1}uh) \quad (20)$$

The values of a proper random function on a polyhedron with geometrical symmetry group M should not distinguish between different orientations eqs. 19 and 20 within the same

l	\mathcal{C}_2	D_2	\mathcal{C}_3	D_3	\mathcal{C}_4	D_4	\mathcal{C}_6	D_6	T	O	\mathcal{J}
0	1	1	1	1	1	1	1	1	1	1	1
1	1	0	1	0	1	0	1	0	0	0	0
2	3	2	1	1	1	1	1	1	0	0	0
3	3	1	3	1	1	0	1	0	1	0	0
4	5	3	3	2	3	2	1	1	1	1	0
5	5	2	3	1	3	1	1	0	0	0	0
6	7	4	5	3	3	2	3	2	2	1	1

Table 3: The multiplicity $m(\Gamma_1 \downarrow l)$ for the values l , $0 \leq l \leq 6$ of the multipole order and selected point groups M in the notation of [22], assuming a function invariant under M . Most numbers are from [22] pp. 436-438, the last column from eq. 44.

geometrical shape. It follows that the two random functions eq. 19 and eq. 20 must coincide. Applying this argument to all elements of M it follows that the random function $\Psi^{\text{random}}(u)$ must be M -invariant with domain the conical section described before Prop 3.

Now we can infer selection rules for the multipole expansion of this random function. For use in molecular physics, the relation between point symmetry and total rotational angular momentum is well studied. Listed for example in [22], pp. 436-438, is the multiplicity $m(l, \downarrow \Gamma_p)$ of the representation Γ_p , $p = 1, 2, \dots$ of the point group M of a molecule contained in the representation D^l , $l = 0, 1, 2, \dots$ of the rotation group. From Frobenius reciprocity, see [7] p. 86, it follows that the multiplicity $m(\Gamma_p \uparrow l)$ of linearly independent functions, constructed from a function belonging to the representation Γ_p of the point group M and transforming under rotations according to D^l , obeys

$$m(\Gamma_p \uparrow l) = m(l \downarrow \Gamma_p). \quad (21)$$

This rule applies in particular to the identity representation Γ_1 of the point group M . The random function $\Psi^{\text{random}}(u)$ eq. 20 is assumed to be M -invariant and so belongs to the representation Γ_1 of M . Application of eq. 21 gives

Prop 4: A random function $\Psi^{\text{random}}(u)$ on a (spherical) polyhedral topological 3-manifold, invariant under its point group M , can contribute to the multipole order l only if $m(l \downarrow \Gamma_1) \geq 1$.

A direct proof of this proposition follows by use of eqs. 16, 18: For given multipole order l , the projector to the identity representation Γ_1 of the rotational polyhedral symmetry group M acts only on the spherical harmonics $Y_m^l(\theta, \phi)$. It gives a non-vanishing result only if $m(l \downarrow \Gamma_1) \geq 1$. In the Table 3, adapted from [22], we collect the relevant numbers $m(l \downarrow \Gamma_1)$ for some point groups up to multipole order $l = 6$. Recursive results for higher values of l are given in the same reference.

Clearly the assumption of random polyhedral point symmetry, combined with homotopy, yields strong multipole selection rules. For the Platonic polyhedral 3-manifolds studied

here we find: The tetrahedron has lowest multipole orders $l = 0, 3, 4, 6^2$, the cube and octahedron lowest multipole orders $l = 0, 4, 6$, the dodecahedron and icosahedron lowest multipole orders $l = 0, 6$. In Appendix C we exemplify the deck and point groups and the onset of invariant polynomials for the cubic manifold $N3$, and in section A.1 we give selection rules from point symmetry for the tetrahedral manifold $N1$.

7 Summary.

We summarize here the salient points of the present work, which to our knowledge are not covered in the work on cosmic topology published by other authors:

(1) **Platonic topologies:** We deal mainly with the family of Platonic spherical 3-manifolds whose homotopies have recently been derived in [11]. Harmonic analysis on these manifolds with homotopies given in [11] is not available from other sources. A great deal of our general methods apply to non-Platonic polyhedral 3-manifolds.

(2) **Start from the fundamental group:** The starting point taken for each spherical 3-manifold is its fundamental or first homotopy group. We remove any ambiguity in the group action by always starting from the geometry and the fundamental group of the polyhedral manifold. The only remaining freedom is the orientation of the quadruple of Weyl vector for the associated Coxeter group Γ . This freedom must be explored as the frame dependence of the modelization, point (9). By an elementwise rigorous conversion of homotopy groups we construct the isomorphic group H of deck transformations. On this basis we derive left, right, or two-sided actions of H on S^3 . Our distinction of these actions agrees with the one used in [23].

(3) **Inequivalent topologies from a single polyhedron:** The work [11] lists inequivalent homotopy groups for a chosen Platonic polyhedron. We follow [11] and give for spherical cubes two inequivalent groups, illustrated in 5, for spherical octahedra three inequivalent groups H of homotopies, isomorphic groups of deck transformations, and bases for the harmonic analysis. The harmonic bases differ in their homotopic boundary conditions.

(4) **Algebraic harmonic analysis and homotopic boundary conditions:** The harmonic analysis is developed on the universal cover S^3 . We use the Wigner harmonic polynomials, Appendix B, which form a complete orthonormal basis on the domain S^3 . The basis for the harmonic analysis on a spherical manifold is constructed by most other authors in the field by numerical methods, see for example [1] p.9 or [25]. For the Platonic 3-manifolds we always proceed algebraically by use of group representations. The bases are spanned by the H -invariant subsets of Wigner polynomials on the 3-sphere. In particular for the manifolds $N1 - N4$, Wigner polynomials give extremely simple results.

We show in section 3.2 that the basis functions of the harmonic analysis obey boundary conditions on pairs of polyhedral faces and so reflect the chosen homotopy.

(5) **Group/subgroup analysis:** The selection rules for a specific 3-manifold we illuminate by representations of groups intermediate between the rotation group $O(4, R)$ and the specific group H of deck transformations. We put the group H , the Coxeter group Γ , and

its unimodular subgroup $S\Gamma$ into the subgroup relation $H < S\Gamma < SO(4, R)$. Selection rules from the representations of these groups we derive in particular for the tetrahedral manifold $N1$, see [18] and Table 5, and for the two cubic manifolds $N2, N3$, see [19]. Even stronger selection rules result from the assumption of random point symmetry in Appendix C.

(6) **Algebraic multipole analysis:** By an algebraic transformation, combined with a transformation of angular coordinates given in sections 6.1-2, we adapt the Wigner polynomials to an explicit multipole expansion with standard transformation properties eq. 16 under rotations, as used in observing the CMB.

(7) **Anisotropy:** We point out two sources of anisotropy. The first one comes from the orientation of the polyhedral prototile, the second one, exemplified by the tetrahedral, cubic and octahedral manifolds, reflects the boundary conditions of the harmonic analysis set by homotopy.

(8) **From random point symmetry to multipole selection rules:** We show in section 6.6 that the additional assumption of random geometrical polyhedral point symmetry, in conjunction with homotopy of the polyhedral manifold, implies strong multipole selection rules for CMB radiation. We emphasize that similar selection rules from deck and random point symmetry apply to regular polyhedral topologies of hyperbolic and Euclidean type.

Acknowledgment.

The author appreciates substantial general advice and help in algebraic computations by Dr. Tobias Kramer, Institut für Theoretische Physik der Universität Regensburg, Germany.

A Synopsis of Platonic polyhedral manifolds.

In this section we illustrate in figures the polyhedra in relation to Coxeter groups and the enumeration of faces and edges, elaborate for the seven spherical Platonic spherical 3-manifolds listed in Table 1, the homotopy in terms of face and edge gluings, the groups H of deck transformations and their action on S^3 , and the basis for the harmonic analysis in terms of Wigner polynomials.

A.1 The tetrahedral manifold $N1$.

The Coxeter group $\Gamma = \circ - \circ - \circ - \circ$ is isomorphic to the symmetric group $S(5)$ of order $|\Gamma| = 5! = 120$. On S^3 it has 120 Coxeter simplices. Sets of 24 of them, each sharing a single vertex, form 5 tetrahedra, Fig. 2. The four Weyl generators of $\Gamma = S(5)$ correspond to the four permutations $(1, 2), (2, 3), (3, 4), (4, 5)$ written in cycle form.

The tetrahedra tile S^3 and form the 5-cell tiling [28] p. 170. In Fig. 3 we show the enumeration of faces and directed edges of the tetrahedron.

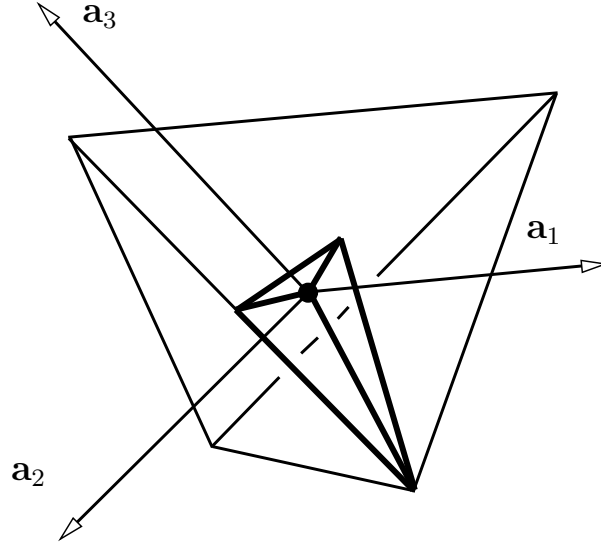


Figure 2: The Weyl vectors a_1, a_2, a_3 of the Coxeter group $\Gamma = \circ - \circ - \circ - \circ$, and the Coxeter simplex bounded by the Weyl reflection planes. 24 Coxeter simplices share a vertex and form the tetrahedral manifold $N1$. In Figs. 2-8 we replace the Platonic spherical polyhedra by their Euclidean counterparts.

Face gluings.

$$F3 \cup F1, F2 \cup F4. \tag{22}$$

Edge gluing scheme. In this and in the corresponding schemes for other manifolds, directed edges in a single horizontal line are glued.

$$\begin{bmatrix} 1 & \bar{3} & \bar{4} \\ 2 & \bar{5} & \bar{6} \end{bmatrix} \tag{23}$$

The combination of the given face and edge gluings fully determines the generators of the fundamental group.

Group $H = \text{deck}(N1)$.

The group $H = \text{deck}(N1)$ of deck transformations from [18] is the cyclic group C_5 . Its generator is given in Table 4.

For the generator of deck transformations of the tetrahedron we deviate from the gluing prescription of [11]. Instead of the generator g_1 from [11] for the face gluing $F3 \cup F1$ we prefer in Table 4 the cyclic permutation $(1, 2, 3, 4, 5)$. The action of its inverse is illustrated in Fig. 4. It can be shown in terms of permutations in cycle form, that $g_1 = (1, 3, 5, 4, 2) = (3, 5, 2)(1, 2, 3, 4, 5)(2, 5, 3)$ so that g_1 prescribed by [11] is conjugate in Γ to the present choice.

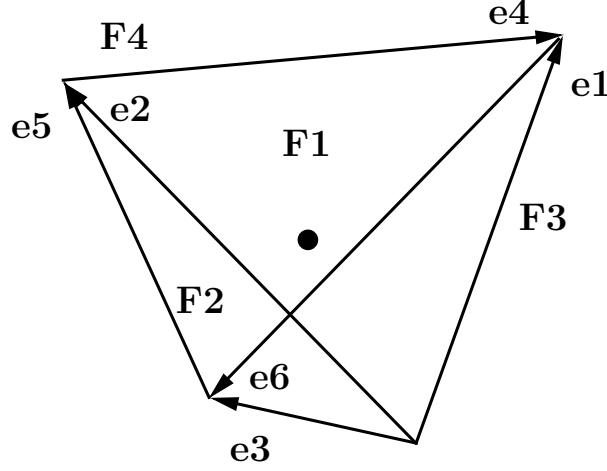


Figure 3: Enumeration of the four faces F_s and six directed edges e_j of the tetrahedral spherical manifold from [11].

The subgroups in $O(4, R) > S(5) > C_5$ and their reduction are implemented in [18]. In the next Table, a corrected version of Table 4.9 from [18], we give the multiplicity analysis with these subgroups for $0 \leq 2j \leq 10$. The representations of $S(5)$ are characterized by partitions f . The Table shows that the representations of $S(5)$ with partitions $f = [41], [2111]$ do not contribute C_5 -invariant polynomials. If random tetrahedral point symmetry is assumed as suggested in 6.6 and carried out for the manifold $N2$ in C , one must look for polynomials invariant under $S\Gamma = A(5)$. The corresponding representations arise only from the partitions $[5]$ and $[11111]$ of $S(5)$. Table 5 shows that then the total multiplicity of invariant polynomials under $A(5)$ for polynomial degrees $2j \leq 10$ reduces from 101 to 13.

$$T_{(W_1W_2W_3W_4)} = T_{(g_l, g_r)},$$

$$g_l = v_1v_2^{-1}v_3v_4^{-1} = \begin{bmatrix} \frac{2+2\sqrt{5}+i(-\sqrt{2}+\sqrt{10})}{8} & \frac{3\sqrt{2}+\sqrt{10}+i(-6+2\sqrt{5})}{8\sqrt{3}} \\ -\frac{3\sqrt{2}+\sqrt{10}+i(6-2\sqrt{5})}{8\sqrt{3}} & \frac{2+2\sqrt{5}+i(\sqrt{2}-\sqrt{10})}{8} \end{bmatrix},$$

$$g_r = v_1^{-1}v_2v_3^{-1}v_4 = \begin{bmatrix} \frac{2-2\sqrt{5}-i(\sqrt{2}+\sqrt{10})}{8} & -\frac{3\sqrt{2}+\sqrt{10}+i(6+2\sqrt{5})}{8\sqrt{3}} \\ -\frac{3\sqrt{2}+\sqrt{10}+i(-6-2\sqrt{5})}{8\sqrt{3}} & \frac{2-2\sqrt{5}+i(\sqrt{2}+\sqrt{10})}{8} \end{bmatrix}.$$

Table 4: ($N1a$) The generator of the cyclic group $H = C_5$ of deck transformations for the spherical tetrahedron. This generator corresponds to the product of the four generating Weyl reflections. The table is constructed by use of eq. 11.

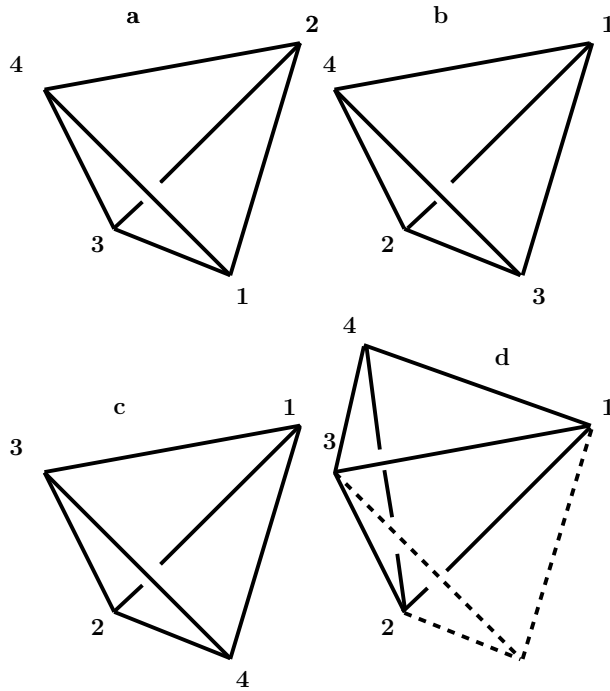


Figure 4: The action of the inverse generator $(W_4W_3W_2W_1) = (5, 4, 3, 2, 1)$ of C_5 , taken as a cyclic permutation from $\Gamma = S(5)$. The vertices of the tetrahedral prototile are denoted by $(1, 2, 3, 4)$. Shown is the factorization of this generator into Weyl reflections. a: initial tetrahedron T , b: $(W_2W_1)T$, c: $(W_3W_2W_1)T$, d: $(W_4W_3W_2W_1)T$. The reflection plane for W_4 contains the vertices $(1, 2, 3)$ in c and d. W_4 in d reflects the tetrahedron shown in c from the dashed into the undashed position.

Basis of harmonic analysis. Here we present a new approach to the C_5 -invariant basis by reducing directly between the groups $SO(4, R) > C_5$. We first diagonalize the matrices (g_l, g_r) eq. 24 in the forms

$$g_l = c_l \delta_l c_l^\dagger, \quad g_r = c_r \delta_r c_r^\dagger. \quad (24)$$

where the diagonal entries of δ_l, δ_r are found from the traces of (g_l, g_r) eq. 24 as $\lambda_l = \exp(\pm \frac{2i\pi}{5})$, $\lambda_r = \exp(\pm \frac{6i\pi}{5})$. Upon transforming the coordinates u from eq. 1 by

$$u \rightarrow u' = c_l^\dagger u c_r, \quad (25)$$

the Wigner polynomials $D^j(u')$ as functions of the new coordinates transform under C_5 by actions from left and right of diagonal 2×2 matrices as

$$u' \rightarrow \delta_l^{-1} u' \delta_r. \quad (26)$$

Under this substitution, the Wigner polynomials from eqs. 14, 24 transform as

$$D_{m_1 m_2}^j(u') \rightarrow D_{m_1 m_2}^j(\delta_l^{-1} u' \delta_r) = \exp(i(-m_1 + 3m_2) \frac{2\pi}{5}) D_{m_1 m_2}^j(u'). \quad (27)$$

$f :$	[5]	[1111]	[41]	[2111]	[32]	[221]	[311]	$m'((j,j),0)$
$(2j)$								
0	1							1
1			1					0
2			1		1			1
3	1		1		1		1	4
4	1		2		1	1	1	5
5	1		2		2	1	2	8
6	1		3	1	3	1	2	9
7	1		4	1	3	2	3	12
8	2		4	1	4	3	4	17
9	2		5	2	5	3	5	20
10	2	1	6	2	6	3	6	24
$\nu_0(f)$	12	1	0	0	26	14	48	101

Table 5: (N1b) Multiplicities $m((j,j),f)$ in the reduction of representations $D^{(j,j)} = \sum_j m((j,j),f)D^f$ from $O(4,R)$ to $S(5)$ as function of $(2j) = 0, \dots, 10$ and of all partitions f . $m'((j,j),0)$ in the last column denotes the total number of C_5 -invariant modes for fixed $(2j)$, $\nu_0(f)$ in the last row those for a fixed partition f up to $(2j) = 10$.

$\psi_{m_1 m_2}^j(u')$	$\delta_{-m_1+3m_2, 0 \bmod 5} D_{m_1 m_2}^j(u'), 2j = 0, 1, 2, \dots - j \leq (m_1, m_2) \leq j.$
------------------------	--

Table 6: (N1c) The C_5 -invariant basis of harmonic analysis for the tetrahedral manifold N1 in terms of Wigner polynomials.

Projection to the identity representation of C_5 from this equation requires

$$-m_1 + 3m_2 \equiv 0 \bmod 5. \quad (28)$$

This selection rule yields the basis of the harmonic analysis of the manifold N1 in Table 6.

A.2 The cubic manifolds N2 and N3.

The Coxeter group $\Gamma = \circ - \overset{4}{\circ} - \circ - \circ$ has $|\Gamma| = 384$ simplices on S^3 . Sets of 48 of them sharing a single vertex form the 8 cubes, Fig. 5, of the 8-cell tiling [28] pp. 170-171. In Fig. 6 we show the enumeration of faces and edges of the cube. The generated groups of deck transformations from [19] are a cyclic group $H = C_8$ for N2 and the quaternion group Q for N3.

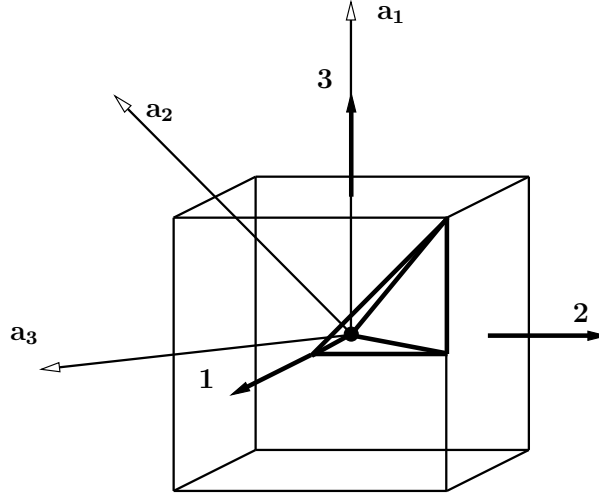


Figure 5: The unit vectors 1, 2, 3, the Weyl vectors a_1, a_2, a_3 of the Coxeter group $\Gamma = \circ - \circ - \circ - \circ$, and the Coxeter simplex bounded by the Weyl reflection planes. 48 Coxeter simplices share a vertex and form the cubic manifolds $N2, N3$.

Cubic manifold $N2$.

Face gluings. After correction of an error in [19] eq. 9,

$$F3 \cup F1, F4 \cup F2, F6 \cup F5. \quad (29)$$

Edge gluing scheme. Directed edges in a single line are glued.

$$\begin{bmatrix} 1 & 3 & 4 \\ 2 & 6 & \overline{9} \\ 5 & 7 & \overline{10} \\ 8 & 11 & \overline{12} \end{bmatrix} \quad (30)$$

Group $H = \text{deck}(N2)$.

The group $H = \text{deck}(N2)$ is the cyclic group C_8 generated by the elements in Table 7. The projector eq. 7 for the manifold $N2$ is given in [19].

Basis of harmonic analysis: Given in Table 8.

Cubic manifold $N3$.

Face gluings. Opposite faces of the cube are glued,

$$F1 \cup F6, F2 \cup F4, F3 \cup F5. \quad (31)$$

t	$(g_l)^t x$	$(g_l)^t$	$(g_r)^t$
1	$(x_1, -x_3, x_0, x_2)$	$\begin{bmatrix} -\bar{a} & 0 \\ 0 & -a \end{bmatrix}$	$\begin{bmatrix} 0 & -a^3 \\ -a & 0 \end{bmatrix}$
2	$(-x_3, -x_2, x_1, x_0)$	$\begin{bmatrix} \bar{a}^2 & 0 \\ 0 & a^2 \end{bmatrix}$	$\begin{bmatrix} -1 & 0 \\ 0 & -1 \end{bmatrix}$
3	$(-x_2, -x_0, -x_3, x_1)$	$\begin{bmatrix} -\bar{a}^3 & 0 \\ 0 & -a^3 \end{bmatrix}$	$\begin{bmatrix} 0 & a^3 \\ a & 0 \end{bmatrix}$
4	$(-x_0, -x_1, -x_2, -x_3)$	$\begin{bmatrix} -1 & 0 \\ 0 & -1 \end{bmatrix}$	$\begin{bmatrix} 1 & 0 \\ 0 & 1 \end{bmatrix}$
5	$(-x_1, x_3, -x_0, -x_2)$	$\begin{bmatrix} \bar{a} & 0 \\ 0 & a \end{bmatrix}$	$\begin{bmatrix} 0 & -a^3 \\ -a & 0 \end{bmatrix}$
6	$(x_3, x_2, -x_1, -x_0)$	$\begin{bmatrix} -\bar{a}^2 & 0 \\ 0 & -a^2 \end{bmatrix}$	$\begin{bmatrix} -1 & 0 \\ 0 & -1 \end{bmatrix}$
7	$(x_2, x_0, x_3, -x_1)$	$\begin{bmatrix} \bar{a}^3 & 0 \\ 0 & a^3 \end{bmatrix}$	$\begin{bmatrix} 0 & a^3 \\ a & 0 \end{bmatrix}$
8	(x_0, x_1, x_2, x_3)	$\begin{bmatrix} 1 & 0 \\ 0 & 1 \end{bmatrix}$	$\begin{bmatrix} 1 & 0 \\ 0 & 1 \end{bmatrix}$

Table 7: (*N2a*) The elements of the cyclic group $H = \text{deck}(N2) = C_8$ of deck transformations of the manifold $N2$ and their actions on S^3 , with $a = \exp(\pi i/4)$.

$j = \text{integer}, m_1 = \text{even}, -j \leq m_1 \leq j, i^{m_1}(-1)^j = 1, m_2 = 0 :$
$\phi_{m_1,0}^j = \frac{\sqrt{2j+1}}{\sqrt{8\pi}} D_{m_1,0}^j(u),$
$j = \text{integer}, m_1 = \text{even}, -j \leq m_1 \leq j, 0 < m_2 \leq j :$
$\phi_{m_1,m_2}^j = \frac{\sqrt{2j+1}}{4\pi} [D_{m_1,m_2}^j(u) + i^{m_1}(-1)^{(j+m_2)} i^{m_2} D_{m_1,-m_2}^j(u)]$

Table 8: (*N2b*) The $H = C_8$ -periodic basis $\{\phi_{m_1,m_2}^j\}$ on S^3 for the harmonic analysis on the cubic spherical 3-manifold $N2$ in terms of Wigner polynomials $D^j(u)$ on S^3 .

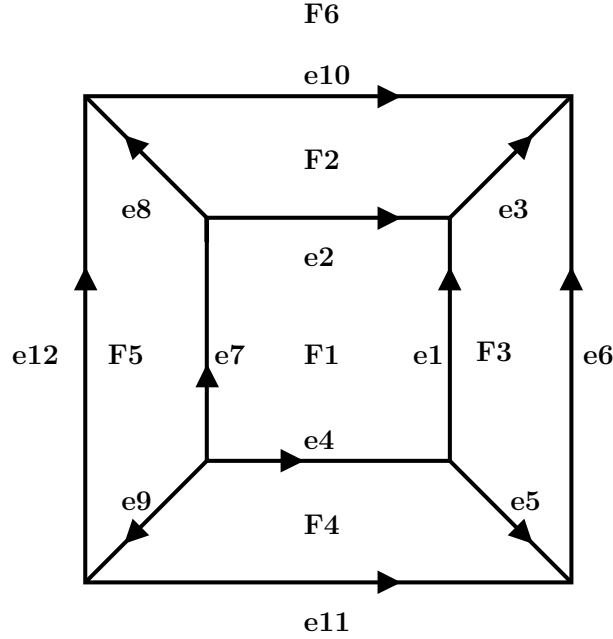


Figure 6: Enumeration of faces $F1, \dots, F6$ and edges $e1, \dots, e12$ for the cubic prototile according to Everitt [11] p. 260 Fig. 2.

Edge gluing scheme. Directed edges in a single line are glued.

$$\begin{bmatrix} 1 & 8 & 11 \\ 2 & \overline{6} & \overline{9} \\ 3 & 4 & \overline{12} \\ 5 & \overline{7} & \overline{10} \end{bmatrix} \quad (32)$$

Group $H = \text{deck}(N3)$

We construct three glue generators q_1, q_2, q_3 in Table 9 from the prescription of [11] p. 259 Table 3. The group H is the quaternionic group Q [9] p. 134. It acts exclusively by left action.

The projector eq. 7 acting on Wigner polynomials from [19] gives

$$(P_Q^0 D_{m_1, m_2}^j)(u) = \frac{1}{8} [1 + (-1)^{2j}] [1 + (-1)^{m_1}] [D_{m_1, m_2}^j(u) + (-1)^j D_{-m_1, m_2}^j(u)]. \quad (33)$$

Basis of harmonic analysis: Given in Table 10.

i	$q_i x$	g_{li}	g_{ri}
1	$(x_1, -x_0, x_3, -x_2)$	$\begin{vmatrix} 0 & -i \\ -i & 0 \end{vmatrix} = -\mathbf{k}$	e
2	$(x_2, -x_3, -x_0, x_1)$	$\begin{vmatrix} 0 & -1 \\ 1 & 0 \end{vmatrix} = -\mathbf{j}$	e
3	$(x_3, x_2, -x_1, -x_0)$	$\begin{vmatrix} -i & 0 \\ 0 & i \end{vmatrix} = -\mathbf{i}$	e

Table 9: ($N3a$) The three generators q_i of the quaternionic group $H = \text{deck}(N3) = Q$ as elements of the Coxeter group Γ and the corresponding pairs $(g_{li}, g_{ri}) \in (SU^l(2, R) \times SU^r(2, R))$. Products of the matrices $\mathbf{i}, \mathbf{j}, \mathbf{k}$ follow the standard quaternionic rules.

$j = \text{odd}, j \geq 3, m_1 = \text{even}, 0 < m_1 \leq j, -j \leq m_2 \leq j :$
$\phi_{m_1, m_2}^{j\text{odd}} = \frac{\sqrt{2j+1}}{4\pi} [D_{m_1, m_2}^j(u) - D_{-m_1, m_2}^j(u)] ,$ $m(Q(j, j), 0) = \frac{1}{2}(2j+1)(j-1),$
$j = \text{even}, m_1 = 0, -j \leq m_2 \leq j :$
$\phi_{0, m_2}^{j\text{even}} = \frac{\sqrt{2j+1}}{\sqrt{8\pi}} D_{0, m_2}^j(u),$
$j \geq 2, \text{even}, 0 < m_1 \leq j, m_1 = \text{even} :$
$\phi_{m_1, m_2}^{j\text{even}} = \frac{\sqrt{2j+1}}{4\pi} [D_{m_1, m_2}^j(u) + D_{-m_1, m_2}^j(u)] ,$ $m(Q(j, j), 0) = \frac{1}{2}(2j+1)(j+2)$

Table 10: ($N3b$) The Q -invariant orthonormal basis $\{\phi_{m_1, m_2}^{j\text{odd}}, \phi_{m_1, m_2}^{j\text{even}}\}$ for the harmonic analysis on the cubic spherical manifold $N3$ in terms of Wigner polynomials $D^j(u)$ on S^3 .

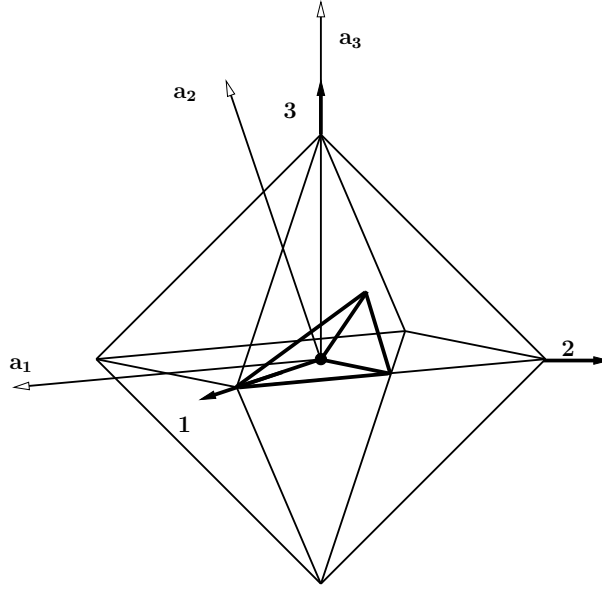


Figure 7: The unit vectors 1, 2, 3, the Weyl vectors a_1, a_2, a_3 of the Coxeter group $\Gamma = \circ - \circ - \circ - \circ$, and the Coxeter simplex bounded by the Weyl reflection planes. 48 Coxeter simplices share a vertex and form the octahedral manifolds N_4, N_5, N_6 .

A.3 The octahedral manifolds N_4, N_5, N_6 .

The Coxeter group $\Gamma = \circ - \circ - \circ - \circ$ has $|\Gamma| = 1152$ simplices on S^3 . Sets of 48 of them sharing a single vertex form the 24 octahedra, Fig. 7, of the 24-cell tiling [28] pp. 171-172. The homotopies of the octahedral 3-manifolds given in [11] were corrected in part in [6]. Face and edge enumerations are given in Fig. 8.

The groups of deck transformations from [20] are the direct product $H = C_3^l \times Q^r$ for N_4 , a group $H = B$ for N_5 , and the binary tetrahedral group \mathcal{T}^* for N_6 . The generators of these groups are given in Tables 11, 12, 14.

Octahedral manifold N_4 .

Face gluings:

$$F_6 \cup F_2, F_5 \cup F_3, F_1 \cup F_4, F_7 \cup F_8. \quad (34)$$

Edge gluing scheme:

$$\begin{bmatrix} 1 & 4 & 9 \\ 2 & 7 & \overline{12} \\ 3 & 6 & \overline{10} \\ 5 & 8 & 11 \end{bmatrix} \quad (35)$$

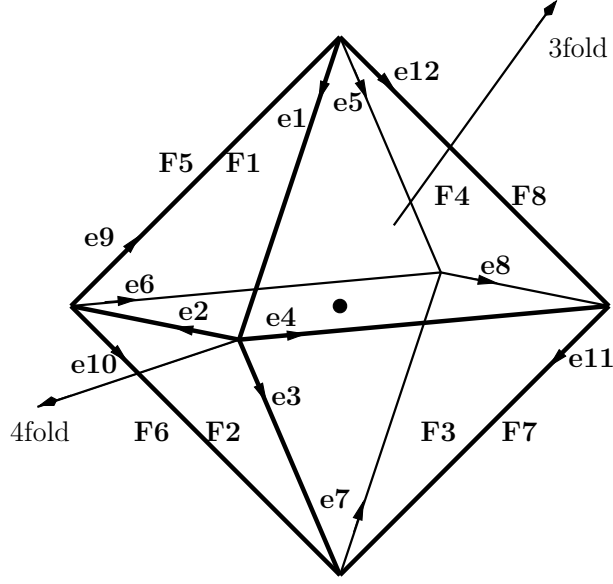


Figure 8: The octahedron projected to the plane with faces $F1 \dots F8$ and directed edges $e1 \dots e12$ according to [11]. The products of Weyl reflections (W_1W_2) and (W_2W_3) generate right-handed 3fold and 4fold rotations respectively.

Group $H = \text{deck}(N4)$.

The group $H = \text{deck}(N4)$ is a direct product $H = C_3^l \times Q^r$ where the upper indices stand for left and right actions. For the projection to a H -periodic basis of $N4$ we first diagonalize the generator $-\alpha_2 \in C_3^l$ given in Table 16,

$$-\alpha_2 = c \begin{bmatrix} \exp(\frac{2\pi i}{3}) & 0 \\ 0 & \exp(-\frac{2\pi i}{3}) \end{bmatrix} c^\dagger, \quad (36)$$

$$c = \begin{bmatrix} (1-i)\frac{-1+\sqrt{3}}{2\sqrt{3-\sqrt{3}}} & -(1-i)\frac{1+\sqrt{3}}{2\sqrt{3+\sqrt{3}}} \\ \frac{1}{\sqrt{3-\sqrt{3}}} & \frac{1}{\sqrt{3+\sqrt{3}}} \end{bmatrix}.$$

Similar as was done for the tetrahedral manifold, we interpret the substitution $u \rightarrow u' = c^\dagger u$ as a transformation to new coordinates u' and derive the basis in these new coordinates. All elements of the group C_3^l are now diagonal in the new coordinate basis. Projection to the identity representation then gives the result of Table 13.

From these generators we derive the structure of the group $H = C_3^l \times Q^r$ with elements given in Table 12.

Basis of harmonic analysis: Given in Table 13.

g	g_l	g_r
g_1	$-\alpha_2$	μ
g_2	$-\alpha_2^{-1}$	$-e$
g_3	α_2	ν
g_4	α_2^{-1}	ω

Table 11: ($N4a$) Generators $g = (g_l, g_r)$ of $\text{deck}(N4)$. We use the short-hand notation of Table 16.

subgroup	elements (g_l, g_r)
C_3^l	$(-\alpha_2, e), ((\alpha_2)^2, e), ((-\alpha_2)^3, e) = (e, e)$
Q^r	$(e, \pm e), (e, \pm\mu), (e, \pm\nu), (e, \pm\omega)$

Table 12: ($N4b$) The elements $g = (g_l, g_r)$ of the group $\text{deck}(N4) = C_3^l \times Q^r$ in the notation of Table 16.

$j = \text{odd}, j \geq 3, m_2 = \text{even}, 0 < m_2 \leq j, m_1 = \rho \equiv 0 \pmod{3} :$
$\phi_{\rho, m_2}^{j \text{ odd}} = [D_{\rho, m_2}^j(u') - D_{\rho, -m_2}^j(u')],$
$j = \text{even}, m_2 = 0, m_1 = \rho \equiv 0 \pmod{3} :$
$\phi_{\rho, 0}^{j \text{ even}} = D_{\rho, 0}^j(u')$
$j \geq 2, \text{even}, 0 < m_2 \leq j, m_2 = \text{even}, m_1 = \rho \equiv 0 \pmod{3} :$
$\phi_{\rho, m_2}^{j \text{ even}} = [D_{\rho, m_2}^j(u') + D_{\rho, -m_2}^j(u')]$

Table 13: ($N4c$) The $(C_3^l \times Q^r)$ -periodic basis for the manifold $N4$ in terms of Wigner polynomials D^j . Only integer values of j appear. The coordinate transform $u \rightarrow u' = c^\dagger u$ in $D^j(u)$ follows with c from eq. 36.

s	g_l	g_r	$g_l^{-1}g_r$
± 1	α_2^{-1}	$\mp\nu$	$\pm\alpha_1$
± 2	α_2^{-1}	$\pm e$	$\pm\alpha_2$
± 3	α_2	$\pm\nu$	$\pm\alpha_3$
± 4	$\sqrt{\frac{1}{2}} \begin{bmatrix} -i & -1 \\ 1 & i \end{bmatrix}$	$\pm\sqrt{\frac{1}{2}} \begin{bmatrix} 1 & -1 \\ 1 & 1 \end{bmatrix}$	$\pm\alpha_4$
± 5	$\sqrt{\frac{1}{2}} \begin{bmatrix} -i & -1 \\ 1 & i \end{bmatrix}$	$\mp\sqrt{\frac{1}{2}} \begin{bmatrix} 1 & 1 \\ -1 & 1 \end{bmatrix}$	$\pm\alpha_1^{-1}$
± 6	α_2	$\pm e$	$\pm\alpha_2^{-1}$
± 7	$\begin{bmatrix} 0 & \theta \\ -\theta & 0 \end{bmatrix}$	$\mp\sqrt{\frac{1}{2}} \begin{bmatrix} 1 & -1 \\ 1 & 1 \end{bmatrix}$	$\pm\alpha_3^{-1}$
± 8	$\begin{bmatrix} 0 & \theta \\ -\theta & 0 \end{bmatrix}$	$\pm\sqrt{\frac{1}{2}} \begin{bmatrix} 1 & 1 \\ -1 & 1 \end{bmatrix}$	$\pm\alpha_4^{-1}$
± 9	e	$\pm e$	$\pm e$
± 10	$-\sqrt{\frac{1}{2}} \begin{bmatrix} i & i \\ i & -i \end{bmatrix}$	$\pm\sqrt{\frac{1}{2}} \begin{bmatrix} 1 & 1 \\ -1 & 1 \end{bmatrix}$	$\pm\mu$
± 11	e	$\pm\nu$	$\pm\nu$
± 12	$\sqrt{\frac{1}{2}} \begin{bmatrix} i & i \\ i & -i \end{bmatrix}$	$\pm\sqrt{\frac{1}{2}} \begin{bmatrix} 1 & -1 \\ 1 & 1 \end{bmatrix}$	$\pm\omega$

Table 14: ($N5a$) Elements $g_j = (g_l, g_r)$, $s = \pm 1, \dots, \pm 12$ of the group $B = \text{deck}(N5)$, enumerated according to the 24 octahedral center positions $u'' = g_l^{-1}g_r \in S^3$, in the order and notation of Table 16.

Octahedral manifold $N5$.

Face gluings:

$$F6 \cup F8, F1 \cup F4, F2 \cup F7, F3 \cup F5. \quad (37)$$

Edge gluing scheme:

$$\begin{bmatrix} 1 & 4 & 9 \\ 2 & \overline{7} & \overline{12} \\ 3 & 6 & 8 \\ 5 & \overline{10} & 11 \end{bmatrix} \quad (38)$$

Group $H = \text{deck}(N5)$.

For this manifold we denote the group of deck transformations by $H = \text{deck}(N5) =: B$ and give its elements in Table 14.

Basis of harmonic analysis: The projection and multiplicity must be computed with eqs. 7, 8.

g	g_l	g_r
g_1	$\sqrt{\frac{1}{2}} \begin{bmatrix} \theta & \theta \\ -\bar{\theta} & \bar{\theta} \end{bmatrix} := \alpha_1$	e
g_2	$\sqrt{\frac{1}{2}} \begin{bmatrix} \bar{\theta} & \theta \\ -\bar{\theta} & \theta \end{bmatrix} := \alpha_2^{-1}$	e
g_3	$\sqrt{\frac{1}{2}} \begin{bmatrix} \bar{\theta} & -\bar{\theta} \\ \theta & \theta \end{bmatrix} := \alpha_4^{-1}$	e
g_4	$\sqrt{\frac{1}{2}} \begin{bmatrix} \theta & -\bar{\theta} \\ \theta & \bar{\theta} \end{bmatrix} := \alpha_3$	e

Table 15: ($N6a$) Generators $g = (g_l, g_r)$ of $\text{deck}(N6)$, compare Table 16.

Octahedral manifold $N6$.

Face gluings:

$$F6 \cup F4, F5 \cup F3, F8 \cup F2, F7 \cup F1. \quad (39)$$

Edge gluing scheme:

$$\begin{bmatrix} 1 & 8 & 10 \\ 2 & 5 & 11 \\ 3 & 6 & 12 \\ 4 & 7 & 9 \end{bmatrix} \quad (40)$$

Group $H = \text{deck}(N6)$.

The group $H = \text{deck}(N6)$ is the binary tetrahedral group \mathcal{T}^* .

Using the equivalence $(g_l, g_r) \sim (-g_l, -g_r)$, we have written H entirely in terms of left actions. The group H of homotopies and deck transformations of the 3-manifold $N6$ then turns out to be the binary tetrahedral group $\langle 2, 3, 3 \rangle$ of order 24 in the notation of Coxeter and Moser [9] pp. 134-135. The elements and multiplication rules are given in Tables 16, 17.

The elements in Table 16 obey

$$\begin{aligned} (\alpha_j)^3 = (\alpha_j)^{-3} = -e, \quad \frac{1}{2}\text{Tr}(\alpha_j) = \frac{1}{2}\text{Tr}(\alpha_j^{-1}) = \frac{1}{2}, \quad j = 1, \dots, 4. \\ \mu^2 = \nu^2 = \omega^2 = -e \end{aligned} \quad (42)$$

The last four elements generate as subgroup the quaternion group Q , [9], pp. 134-135. of order 8 with standard elements $\mathbf{i} = -\omega$, $\mathbf{j} = -\nu$, $\mathbf{k} = \mu$.

α_1	α_2	α_3	α_4	
$\sqrt{\frac{1}{2}} \begin{bmatrix} \theta & \theta \\ -\bar{\theta} & \bar{\theta} \end{bmatrix}$	$\sqrt{\frac{1}{2}} \begin{bmatrix} \theta & -\theta \\ \bar{\theta} & \bar{\theta} \end{bmatrix}$	$\sqrt{\frac{1}{2}} \begin{bmatrix} \theta & -\bar{\theta} \\ \theta & \bar{\theta} \end{bmatrix}$	$\sqrt{\frac{1}{2}} \begin{bmatrix} \theta & \bar{\theta} \\ -\theta & \bar{\theta} \end{bmatrix}$	
α_1^{-1}	α_2^{-1}	α_3^{-1}	α_4^{-1}	
$\sqrt{\frac{1}{2}} \begin{bmatrix} \bar{\theta} & -\theta \\ \bar{\theta} & \theta \end{bmatrix}$	$\sqrt{\frac{1}{2}} \begin{bmatrix} \bar{\theta} & \theta \\ -\bar{\theta} & \theta \end{bmatrix}$	$\sqrt{\frac{1}{2}} \begin{bmatrix} \bar{\theta} & \bar{\theta} \\ -\theta & \theta \end{bmatrix}$	$\sqrt{\frac{1}{2}} \begin{bmatrix} \bar{\theta} & -\bar{\theta} \\ \theta & \theta \end{bmatrix}$	(41)
$e, -e$	μ	ν	ω	
$\begin{bmatrix} 1 & 0 \\ 0 & 1 \end{bmatrix}, -\begin{bmatrix} 1 & 0 \\ 0 & 1 \end{bmatrix}$	$\begin{bmatrix} 0 & i \\ i & 0 \end{bmatrix}$	$\begin{bmatrix} 0 & -1 \\ 1 & 0 \end{bmatrix}$	$\begin{bmatrix} -i & 0 \\ 0 & i \end{bmatrix}$	
$e^{-1} = e, (-e)^{-1} = -e$	$\mu^{-1} = -\mu$	$\nu^{-1} = -\nu$	$\omega^{-1} = -\omega$	

Table 16: (*N6b*) The binary tetrahedral group $\mathcal{T}^* \sim \text{deck}(N6)$ has 16 elements $\pm\alpha_j, \pm\alpha_j^{-1}$ and 8 elements $\pm e, \pm\mu, \pm\nu, \pm\omega$, with $\theta = \exp(i\pi/4), \bar{\theta} = \exp(-i\pi/4)$. It acts from the left on $u \in S^3$.

	α_1	α_2	α_3	α_4	α_1^{-1}	α_2^{-1}	α_3^{-1}	α_4^{-1}	μ	ν	ω	e
α_1	$-\alpha_1^{-1}$	α_4	$-\omega$	$-\nu$	e	μ	α_2^{-1}	α_3	$-\alpha_3^{-1}$	α_2	α_4^{-1}	α_1
α_2	α_3	$-\alpha_2^{-1}$	ν	$-\omega$	$-\mu$	e	α_4	α_1^{-1}	α_4^{-1}	$-\alpha_1$	α_3^{-1}	α_2
α_3	μ	$-\omega$	$-\alpha_3^{-1}$	α_1	α_2	α_4^{-1}	e	ν	$-\alpha_4$	$-\alpha_2^{-1}$	α_1^{-1}	α_3
α_4	$-\omega$	$-\mu$	α_2	$-\alpha_4^{-1}$	α_3^{-1}	α_1	$-\nu$	e	α_3	α_1^{-1}	α_2^{-1}	α_4
α_1^{-1}	e	ν	α_4^{-1}	α_2	$-\alpha_1$	α_3^{-1}	$-\mu$	ω	α_2^{-1}	$-\alpha_4$	$-\alpha_3$	α_1^{-1}
α_2^{-1}	$-\nu$	e	α_1	α_3^{-1}	α_4^{-1}	$-\alpha_2$	ω	μ	$-\alpha_1^{-1}$	α_3	$-\alpha_4$	α_2^{-1}
α_3^{-1}	α_4	α_1^{-1}	e	$-\mu$	ω	$-\nu$	$-\alpha_3$	α_2^{-1}	α_1	α_4^{-1}	$-\alpha_2$	α_3^{-1}
α_4^{-1}	α_2^{-1}	α_3	μ	e	ν	ω	α_1^{-1}	$-\alpha_4$	$-\alpha_2$	$-\alpha_3^{-1}$	$-\alpha_1$	α_4^{-1}
μ	$-\alpha_2$	α_1	$-\alpha_1^{-1}$	α_2^{-1}	α_3	$-\alpha_4$	α_4^{-1}	$-\alpha_3^{-1}$	$-e$	$-\omega$	ν	μ
ν	α_4^{-1}	$-\alpha_3^{-1}$	$-\alpha_4$	α_3	$-\alpha_2^{-1}$	α_1^{-1}	α_2	$-\alpha_1$	ω	$-e$	$-\mu$	ν
ω	α_3^{-1}	α_4^{-1}	α_2^{-1}	α_1^{-1}	$-\alpha_4$	$-\alpha_3$	$-\alpha_1$	$-\alpha_2$	$-\nu$	μ	$-e$	ω
e	α_1	α_2	α_3	α_4	α_1^{-1}	α_2^{-1}	α_3^{-1}	α_4^{-1}	μ	ν	ω	e

(43)

Table 17: (*N6c*) Multiplication table for 12 elements g of the binary tetrahedral group $\text{deck}(N6)$ given in Table 16. The 12 elements $-g$ have been suppressed.

Basis of harmonic analysis. The projection and multiplicity must be computed with eqs. 7, 8.

A.4 The dodecahedral manifold $N1'$.

This is the Poincaré dodecahedral manifold analyzed in [16]. The Coxeter group $\circ - \circ - \circ - \circ - \circ$ on S^3 has $|\Gamma| = (120)^2$ simplices. The tiling on S^3 is the 120-cell [28] pp. 176-177. The face gluings for this manifold are well known, see [27] pp. 214-218.

Group $H = \text{deck}(N1')$.

The homotopy group $\pi_1(N1')$ is the binary icosahedral group \mathcal{J}_2 discussed in detail in [14]. In [16] it is transformed into the isomorphic group $H = \text{deck}(N1')$ and related to Hamilton's icosians.

Basis of harmonic analysis: The polynomial basis of the harmonic analysis on this manifold can be constructed for each degree $2j$ by the diagonalization of an operator with explicit matrix representation given in [16], eq.(47) and Appendix. The multiplicity $m(j, 0)$ of \mathcal{J}_2 -invariant basis functions is given from character analysis eq. 8, compare [17], by
(i) the starting values

$$\begin{aligned} j \leq 30 : m(j, 0) &= 1 \text{ for} & (44) \\ j &= 0, 6, 10, 12, 15, 16, 18, 20, 21, 22, 24, 25, 26, 27, 28, \\ m(j, 0) &= 0 \text{ otherwise,} \end{aligned}$$

(ii) the recursion relation

$$m(j + 30, 0) = m(j, 0) + 1. \quad (45)$$

B Wigner polynomials.

The Wigner polynomials are the spherical harmonics on the coset space $SO(4, R)/SU^C(2, C) \sim SU^r(2, C) \sim S^3$, see eq. 4. From [32] pp. 163-166 they are homogeneous of degree $2j$ and given in terms of the complex matrix elements of u from eq. 1 by

$$\begin{aligned} D_{m_1 m_2}^j(z_1, z_2, \bar{z}_1, \bar{z}_2) &= \left[\frac{(j + m_1)!(j - m_1)!}{(j + m_2)!(j - m_2)!} \right]^{1/2} & (46) \\ &\times \sum_{\sigma} \frac{(j + m_2)!(j - m_2)!(-1)^{m_2 - m_1 + \sigma}}{(j + m_1 - \sigma)!(m_2 - m_1 + \sigma)!\sigma!(j - m_2 - \sigma)!} \\ &\times z_1^{j + m_1 - \sigma} \bar{z}_2^{m_2 - m_1 + \sigma} z_2^{\sigma} \bar{z}_1^{j - m_2 - \sigma}, \\ &2j = 0, 1, 2, \dots, -j \leq (m_1, m_2) \leq j. \end{aligned}$$

The summation over σ is restricted by the inverse factorials. The symmetries under inversion and complex conjugation of u are

$$D_{m_1 m_2}^j(u^{-1}) = \overline{D_{m_2 m_1}^j(u)}, \quad \overline{D_{m_1 m_2}^j(u)} = D_{m_1 m_2}^j(\bar{u}) \quad (47)$$

In [16] p. 3526 Lemma 5 it is shown that under the Laplacian Δ on E^4 one has

$$\Delta D_{m_1 m_2}^j(u) = \left(\sum_{i=0}^3 \frac{\partial^2}{\partial x_i^2} \right) D_{m_1 m_2}^j(u) = 0. \quad (48)$$

In other words the Wigner polynomials are harmonic. For the Euler angle parametrization, orthogonality and completeness of the D^j on $S^3 \sim SU(2, C)$ we refer to [32]. The measure of integration on S^3 in terms of the Euler angles is, [10] pp. 62-64,

$$d\mu(\alpha, \beta, \gamma) = d\alpha \sin(\beta) d\beta d\gamma, \quad \int_{SU(2, C)} d\mu(\alpha, \beta, \gamma) = 8\pi^2. \quad (49)$$

C From deck via point to unimodular invariance.

When we introduced in section 6.6 the point group M of a Platonic manifold \mathcal{M} , we did not discuss its relation to the group $\text{deck}(\mathcal{M})$.

In general, the group acts fixpoint-free on S^3 whereas M fixes the center of the prototile. It follows that the two groups have the intersection $\text{deck}(\mathcal{M}) \cap M = e$. Both groups are subgroups of the Coxeter group, and so products of their elements must generate a subgroup of Γ . We place the centers of all prototiles at $x = (1, 0, 0, 0)$. Then the action of a binary point group M^* as a subgroup of the diagonal group $SU^C(2, C)$ with elements of the form $g = (h, h)$, reduces to the ordinary action $R(h)(x_1, x_2, x_3)$ with $R(h) \in M$.

The groups generated from deck and point groups and their projectors can be constructed for each manifold. We exemplify the construction by the cubic spherical manifold $N3$, with H the quaternion group Q , $|Q| = 8$, and M the cubic point group O , $|O| = 24$. The corresponding binary cubic group we denote by O^* .

By explicit computation one finds:

Prop B1: Under conjugation with elements $h \in O^*$, the quaternion group Q is transformed into itself,

$$h \in O^* : h^{-1} Q h = Q. \quad (50)$$

This implies that the group generated from both Q and O is a semidirect group, with Q a normal subgroup.

Prop B2: For the manifold $N3$, the group generated by both $H=Q$ and $M=O$ is the semidirect group

$$G = Q \times_s O, \quad |Q \times_s O| = 8 \times 24 = 192. \quad (51)$$

with elements the products $g = qh$, $q \in Q$, $h \in O^*$.

This is also the order of the unimodular subgroup $S\Gamma$ of the Coxeter group

$\Gamma = \circ \overset{4}{-} \circ - \circ - \circ$ for cubic 3-manifolds from Table 1. It is easy to show that the group $Q \times_s O$ exhausts and so is identical to this subgroup. The unimodular group $S\Gamma = Q \times_s O$ contains the two alternative deck groups for the cubic 3-manifolds $N2$, $N3$, and their cubic point symmetry group O .

We look for the projector to the identity representation of the group $Q \times_s O$. From the semidirect product form eq. 51 there follows:

Prop B3: The projector to the identity representation of $Q \times_s O$ factorizes as

$$P_{Q \times_s O}^0 = \frac{1}{|Q||O|} \sum_{(q_r, h_s, h_s) \in G} T_{(q_r, h_s, h_s)} = P_Q^0 \times P^{\Gamma_1}, \quad (52)$$

$$P^{\Gamma_1} = \frac{1}{|O|} \sum_{h \in O^*} T_{(h, h)}.$$

into the projectors of its two subgroups, with the quaternionic projector given in eq. 33. Here the sum over $h \in O^*$ can be restricted to the 24 elements of O .

We now construct the onset polynomial for the cubic spherical manifold $N3$ under O . From Table 3 it has $j = 2$, $l = 4$. If we go to the alternative basis eq. 15, we can use the classical lowest cubic spherical harmonic, given in [15] pp. 108-109:

$$\psi^{\Gamma_1} = \sqrt{\frac{7}{12}} Y_0^4 + \sqrt{\frac{5}{24}} (Y_4^4 + Y_{-4}^4). \quad (53)$$

Upon using the same linear m -combination in the basis eq. 15, we pass to Wigner polynomials and find

$$\begin{aligned} \psi^{\Gamma_1} = & \sqrt{\frac{7}{12}} [D_{2,2}^2(u) \langle 2 - 222 | 40 \rangle + D_{-2,-2}^2(u) \langle 222 - 2 | 40 \rangle] \\ & + \sqrt{\frac{7}{12}} [D_{1,1}^2(u) \langle 2 - 121 | 40 \rangle (-1) + D_{-1,-1}^2(u) \langle 212 - 1 | 40 \rangle (-1) + D_{0,0}^2(u) \langle 2020 | 40 \rangle] \\ & + \sqrt{\frac{5}{24}} [D_{-2,2}^2(u) \langle 2222 | 44 \rangle + D_{2,-2}^2(u) \langle 2 - 22 - 2 | 4 - 4 \rangle] \end{aligned} \quad (54)$$

The relevant Wigner coefficients can be found from [10] p. 45:

$$\langle 2 \mp 22 \pm 2 | 40 \rangle = \sqrt{\frac{1}{8!}} 4!, \quad \langle 2020 | 40 \rangle = \sqrt{\frac{1}{8!}} 4! 6, \quad \langle 2 \pm 22 \pm 2 | 4 \pm 4 \rangle = 1. \quad (55)$$

Next we follow eq. 15, apply the projector eq. 33 of the quaternion group Q to the poly-

nomial eq. 54, and obtain

$$\begin{aligned}
\psi^{0,\Gamma_1} &= P_Q^0 \psi^{\Gamma_1} = \sqrt{\frac{7}{12}} \left[\frac{1}{2} (D_{2,2}^2(u) + D_{-2,2}^2(u)) \langle 2 - 222 | 40 \rangle \right] \\
&+ \sqrt{\frac{7}{12}} \left[\frac{1}{2} (D_{-2,-2}^2(u) + D_{2,-2}^2(u)) \langle 222 - 2 | 40 \rangle + D_{0,0}^2(u) \langle 2020 | 40 \rangle \right] \\
&+ \sqrt{\frac{5}{24}} \left[\frac{1}{2} (D_{-2,2}^2(u) + D_{2,2}^2(u)) \langle 2222 | 44 \rangle + \frac{1}{2} (D_{2,-2}^2(u) + D_{-2,-2}^2(u)) \langle 2 - 22 - 2 | 4 - 4 \rangle \right]
\end{aligned} \tag{56}$$

where the terms with $m_1 = \pm 1$ in eq. 54 vanish after projection. Upon inserting the Wigner coefficients eq. 55 and combining similar terms, we find for the lowest polynomial of degree 4, invariant under the full group $Q \times_s O = S\Gamma$, the final result

$$\begin{aligned}
\psi^{0,\Gamma_1} &= \sqrt{\frac{3}{10}} \left[\frac{1}{2} [D_{2,2}^2(u) + D_{-2,2}^2(u) + D_{-2,-2}^2(u) + D_{2,-2}^2(u)] + D_{0,0}^2(u) \right] \\
&= \sqrt{\frac{6}{5}} [(x_0^4 + x_1^4 + x_2^4 + x_3^4) - 2(x_0^2 x_1^2 + x_0^2 x_2^2 + x_0^2 x_3^2 + x_1^2 x_2^2 + x_1^2 x_3^2 + x_2^2 x_3^2)].
\end{aligned} \tag{57}$$

The expression in the last line uses eq. 46. It allows to check the invariance both under the deck group Q from Table 9 and under the point group O . Eq. 57 demonstrates the role of the unimodular Coxeter group $S\Gamma$ as the basis underlying **Prop 3**. A similar invariance under both the deck and the point group we discuss in section A.1 for the tetrahedral 3-manifold.

References

- [1] Aurich R, Lustig S, and Steiner F, *CMB anisotropy of the Poincaré dodecahedron*. Class. Quantum Grav. **22** (2005) 2061-83 arXiv:0412569v2
- [2] Aurich R, Lustig S, and Steiner F, *CMB anisotropy of spherical spaces*. Class. Quantum Grav. **22** (2005) 3443-59 arXiv:05046v1
- [3] Aurich R, Janzer H S, Lustig S, and Steiner F, *Do we live in a small universe?* Class. Quantum Grav. **25** (2008) article number 125006 arXiv:0708.1420v2
- [4] Bellon M, *Elements of dodecahedral cosmology*. arXiv:astro-ph/0602076
- [5] Caillerie S, Lachieze-Rey M, Luminet J-P, Lehoucq R, Riazuelo A, and Weeks J, *A new analysis of the Poincaré dodecahedral space model*. arXiv:0706.1559
- [6] Cavicchioli A, Spaggiari F, and Tellone A I, *Topology of compact space forms from Platonic solids.I*. Topology and its Applications **156** (2009), pp. 812-822
- [7] Coleman A J, *Induced and subduced representations*. in: Group Theory and its Applications, ed. E M Loeb, Academic Press, New York 1968
- [8] Copi C J, Huterer D, Schwarz D J, and Starkman G D, *On the large-angle anomalies of the microwave sky*. Mon. Not. Astron. Soc. **000** (2005), 1-27, arXiv:astro-ph/0508047v1
- [9] Coxeter H S M and Moser W O J, *Generators and relations for discrete groups*. Springer, Berlin 1965
- [10] Edmonds A R, *Angular momentum in quantum mechanics*. Princeton University Press, Princeton 1957
- [11] Everitt B, *3-manifolds from Platonic solids*. Topology and its Applications **138** (2004), 253-63
- [12] Hinshaw G et al., *Five-year Wilkinson microwave anisotropy probe observations: Data processing, sky maps, and basic results*. The Astrophys. J Supplement Series **180** (2009), 225-245, 2009
- [13] Humphreys J E, *Reflection groups and Coxeter groups*. Cambridge University Press, Cambridge 1990
- [14] Klein F, *Vorlesungen über das Ikosaeder und die Auflösung der Gleichungen vom fünften Grade*. B G Teubner, Leipzig 1984, Reprint B G Teubner, Leipzig 1993.
- [15] Knox R S and Gold A, *Symmetry in the solid state.*, W A Benjamin, New York 1964

- [16] Kramer P, *An invariant operator due to F Klein quantizes H Poincare's dodecahedral manifold.* J Phys A: Math Gen **38** (2005) 3517-40
- [17] Kramer P, *Harmonic polynomials on the Poincare dodecahedral 3-manifold.* J. of Geometry and Symmetry in Physics **6** (2006) 55-66
- [18] Kramer P, *Platonic polyhedra tune the 3-sphere: Harmonic analysis on simplices.* Physica Scripta **79** (2009) 045008, arXiv:0810.3403
- [19] Kramer P, *Platonic polyhedra tune the 3-sphere II: Harmonic analysis on cubic spherical 3-manifolds.* Physica Scripta **80** (2009) 025902, arXiv:0901.0511
- [20] Kramer P, *Platonic polyhedra tune the 3-sphere III: Harmonic analysis on octahedral spherical 3-manifolds.* Physica Scripta (2010) in print, arXiv:0908.1000v1
- [21] Lachieze-Rey M and Luminet J-P, *Cosmic topology.* Phys Rep **254** (1995) 135-214
- [22] Lax M, *Symmetry principles in solid state and molecular physics.* Wiley, New York (1974)
- [23] Lehoucq R, Weeks J, Uzan J-Ph, Gausmann E, and Luminet J-P, *Eigenmodes of three-dimensional spherical spaces and their application to cosmology.* Cla.. Quantum Grav. **19** (2002) 4683-4708
- [24] Levin J, *Topology and the cosmic microwave background.* Phys Rep **365** (2002) 251-333
- [25] Luminet J-P, Weeks J R, Riazuelo A, Lehoucq R and Uzan J-Ph, *Dodecahedral space topology as an explanation for weak wide-angle temperature correlations in the cosmic microwave background.* Nature **425** (2003) 593-5
- [26] Schwarz D J, *Thoughts on the cosmological principle.* arXiv:0905.0384v1
- [27] Seifert H and Threlfall W, *Lehrbuch der Topologie.* Leipzig 1934, Chelsea Reprint, New York 1980
- [28] Sommerville D M Y, *An introduction to the geometry of N dimensions.* Dover, New York 1958
- [29] Thurston W P, *Three-Dimensional Geometry and Topology.* Princeton University Press, Princeton 1997
- [30] Weeks J, *The Poincaré dodecahedral space and the mystery of the missing fluctuations.* Notices of the AMS **51,6** (2004) 610-19
- [31] Weeks J and Gundermann J, *Dodecahedral topology fails to explain quadrupole-octupole alignment.* Class. Quantum Grav. **2007** 1863-1866

- [32] Wigner E P, *Group theory and its applications to the quantum mechanics of atomic spectra*. Wiley, New York 1959
- [33] Wolf J A, *Spaces of constant curvature*. Publish or Perish Inc., Washington, US 1984, 5th Edition
- [34] Zhang R and Huterer D, *Disks in the sky: A reassessment of the WMAP “cold spot”*. arXiv:0908.3988v1